

# PowerBlade: A Low-Profile, True-Power, Plug-Through Energy Meter

Samuel DeBruin, Branden Ghena, Ye-Sheng Kuo, and Prabal Dutta  
Electrical Engineering and Computer Science Department  
University of Michigan  
Ann Arbor, MI 48109  
[{sdebruin, brghena, samkuo, prabal}@umich.edu](mailto:{sdebruin, brghena, samkuo, prabal}@umich.edu)

## ABSTRACT

We present PowerBlade, the smallest, lowest cost, and lowest power AC plug-load meter that measures real, reactive and apparent power, and reports this data, along with cumulative energy consumption, over an industry-standard Bluetooth Low Energy radio. Achieving this design point requires revisiting every aspect of conventional power meters: a new method of acquiring voltage; a non-invasive, planar method of current measurement; an efficient and accurate method of computing power from the voltage and current channels; a radio interface that leverages nearby smart phones to display data and report it to the cloud; and a retro power supply re-imagined with vastly lower current draw, allowing extreme miniaturization. PowerBlade occupies a mere  $1'' \times 1''$  footprint, offers a  $1/16''$  profile, draws less than 180 mW itself, offers 1.13% error on unity power factor loads in the 2-1200 W range and slightly worse for non-linear and reactive loads, and costs \$11 in modest quantities of about 1,000 units. This new design point enables affordable large-scale studies of plug-load energy usage—an area of growing national importance.

## Categories and Subject Descriptors

B.4.2 [HARDWARE]: Input/Output and Data Communications—*Input/Output Devices*; C.3 [COMPUTER-COMMUNICATION NETWORKS]: Special-Purpose and Application-Based Systems

## General Terms

Design, Experimentation, Measurement, Performance

## Keywords

AC meter, Smart meter, Energy metering, Power metering, Plug-load metering, Data aggregation, Intermittent power, Wireless sensor

Permission to make digital or hard copies of part or all of this work for personal or classroom use is granted without fee provided that copies are not made or distributed for profit or commercial advantage and that copies bear this notice and the full citation on the first page. Copyrights for third-party components of this work must be honored. For all other uses, contact the authors.

Copyright is held by the authors.

*SenSys'15*, November 01–04, 2015, Seoul, Republic of Korea  
ACM 987-1-4503-3631-4/15/11.  
<http://dx.doi.org/10.1145/2809695.2809716>

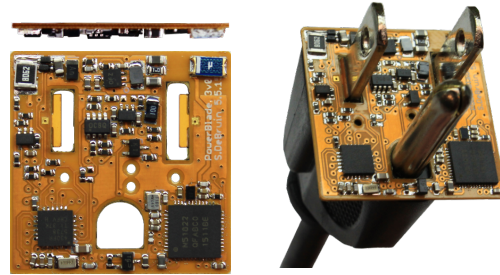


Figure 1: Profile, front, and perspective views of PowerBlade, a wireless power meter that measures real, reactive, and apparent power. PowerBlade's low profile and plug through form factor allow it to sit inconspicuously and unobtrusively between an electrical plug and an outlet, and its square-inch footprint spares adjacent outlets from being blocked. PowerBlade stores accumulated energy data locally and reports both instantaneous power and accumulated energy to a nearby smartphone or gateway over a Bluetooth Low Energy radio.

## 1. INTRODUCTION

Residential and commercial buildings in the US used 2,760 TWh of electrical energy in 2014 [19]. The majority of that usage comes from clearly obvious loads including HVAC, lighting, and appliances, however, approximately a 20% (and growing) share of electricity usage is due to “plug-loads,” often called miscellaneous electrical loads (MELs) in industry terms [27]. These diverse loads, from televisions and computers to vending machines and box fans, represent the long-tail of electricity use. Understanding the characteristics of these loads requires insight into each device’s individual consumption but the methods today are limited. As a result, ratepayers, regulators, and researchers lack the tools to *unobtrusively monitor* plug-load energy use with *high fidelity* and *low cost*.

To help address this problem, we present PowerBlade, a new power/energy meter that achieves a vastly smaller form factor than prior systems. PowerBlade occupies an unobtrusive and essentially two-dimensional volume,  $1'' \times 1'' \times 1/16''$ , and meters loads plugged through it and into an outlet, as Figure 1 shows. Despite its small size, PowerBlade is a wireless true power meter, capable of metering real, reactive, and apparent power at kHz frequencies, aggregating these measurements into cumulative energy, and transmitting these data several times per second using a Bluetooth Low Energy (BLE) radio to a nearby smartphone or gateway. At a cost of \$11 in modest quantities of 1,000 units, PowerBlade is the smallest and lowest cost AC plug-load meter with 1.13% accuracy over a 2-1200 W range for unity power factor loads, and slightly worse for non-linear and reactive loads. This small form factor, coupled with easy access to and transport of the meter data, may enable new applications.

Metering Device	Power Supply	Voltage	Current	True Power?	Data Output	Static Power	Volume
Kill-A-Watt [6]	Capacitor fed	Divider	Resistor	Yes	LCD	450 mW	14.0 in <sup>3</sup>
Watts Up [17]	Capacitor fed	Divider	Resistor	Yes	LCD or USB	590 mW	31.9 in <sup>3</sup>
Belkin Conserve Insight [3]	Capacitor fed	Divider	Resistor	Yes	LCD	440 mW	21.8 in <sup>3</sup>
ACme-A [26]	Capacitor fed	Divider	Resistor	Yes	802.15.4	1000 mW	13.7 in <sup>3</sup>
ACme-B [26]	Transformer	Divider	Hall effect	Yes	802.15.4	100 mW	13.7 in <sup>3</sup>
Monjolo [23]	Energy harvest	None	Current Transformer	No	802.15.4	4 mW	7.8 in <sup>3</sup>
Gemini [20]	Energy harvest	Virtual	Current Transformer	Yes	802.15.4		Not Published
PowerBlade (this work)	Resistor fed	Divider	Magnetometer	Yes	BLE	80-176 mW <sup>†</sup>	0.07 in <sup>3</sup>

Table 1: Comparison of various power meters. PowerBlade is the smallest, lowest power, wireless true power meter. <sup>†</sup>Depends on data rate.

PowerBlade provides an opportunity to think about power metering in a new way. Rather than metering every outlet in a building, PowerBlade is capable of metering every load, following the plug to any outlet with which it mates. This tight binding allows data to be collected about the plug-loads themselves rather than whatever happens to be plugged into an outlet, representing a paradigm shift from prior work that employed bulky power meters. Moreover, existing power meters do not make their data easily accessible to users, but using BLE allows PowerBlade’s measurements to be received by unmodified smartphones. [Section 2](#) provides a more detailed comparison of PowerBlade with existing power meters.

PowerBlade’s small profile and literally plug-through design require revisiting nearly every aspect of power meter design. Since PowerBlade has no outlet of its own, it utilizes exposed conductive tabs built from rigid-flex PCB to make contact with the plug-through AC load. Traditional AC-DC power supplies require substantial volume to hold charge or dissipate power, owing to high load power, but PowerBlade draws less than 6 mW average power itself, allowing it to utilize a small and simple power supply. Conventional current sensing requires breaking the AC path with a sense resistor, encircling it with a current transformer, or monitoring the Hall effect in a plane parallel to the current flow, but these methods are not viable in the PowerBlade design. Rather, PowerBlade measures the magnetic field generated from the current passing through it using a wire-wound inductor optimally placed in the plane perpendicular to the flow of current. This magnetometer design allows the current waveform to be measured using commodity electronic components. These and other design concerns are described in detail in [Section 3](#) and specific implementation choices are presented in [Section 4](#).

PowerBlade offers accurate metering over a wide range of load powers. For resistive loads, such as incandescent bulbs, PowerBlade has an average error of 1.13% over the range of 2 W to 1200 W. We also test the meter on a range of common household loads including a toaster, refrigerator, Xbox, and WiFi router. Across these loads, PowerBlade has an average error of 6.5%. [Section 5](#) provides a detailed evaluation of system accuracy, usability, and safety.

Despite PowerBlade’s small size and high accuracy, we identify several opportunities for future improvements to the system. These include better synchronization between current and voltage channel acquisition, better calculation of power factor, securing the metered data, and providing timestamped and synchronized interval data at the 1, 15, or 60 minute intervals. We discuss these future improvements in [Section 6](#).

With PowerBlade in hand, ratepayers, regulators, and researchers have an increased ability to understand plug-load usage patterns. Large-scale, long-term deployments in residential and commercial settings should lead to greater awareness of plug-load usage and plug-load trends—particularly growing energy waste due to high idle power—providing critical data to regulators for efficiency standards.

## 2. RELATED WORK

A true-power meter performs five distinct functions: (i) reduce the AC mains voltage to low DC voltages to power the meter itself, (ii) measure voltage, (iii) measure current, (iv) calculate power and energy, and (v) communicate these measurements. Scaling a power meter to PowerBlade’s form factor requires revisiting each of these functions as they are all intimately tied to system form factor.

[Table 1](#) presents a sampling of commercial and research meters, and key design choices along the five dimensions that these earlier devices embody. In this section, we survey these systems, noting the effect that these choices have on overall size and power draw. In particular, we survey three commercial meters—Kill-A-Watt [6], Watts Up [17], and Belkin Conserve Insight [3]—and three research meters—ACme [26] (two different versions), Monjolo [23], and Gemini [20]—alongside PowerBlade (this work).

### 2.1 AC-DC Power Supply

For a power meter to operate from the AC mains, it must rectify and step down the AC voltage to provide itself with low voltage DC. Half- or full-wave rectifiers are typically used for this purpose, and they can occupy a small volume using a single or multiple low-profile diodes. Voltage step-down, in contrast, requires more volume and is not blindly amenable to scaling. Moreover, step-down techniques often do not scale as DC power is reduced, requiring a minimum volume regardless of the DC power supplied, while energy harvesters often require bulky current transformers that are fundamentally unsuited to PowerBlade’s form factor [20, 23].

Transformers are the most common step-down technique in “wall wart” power supplies and they are used in the ACme-B design [26]. They are inexpensive, efficient, and isolated devices but their volume does not scale linearly to the form factors needed in our case—the smallest AC transformer available from Coilcraft, for example, is approximately 0.31 in<sup>3</sup> [4], which would dominate our volume.

In capacitor-fed power supplies, a high voltage series capacitor drops the line voltage and limits current. Capacitor-fed power supplies are common in many AC power meters [3, 6, 17, 26] even though they do not provide isolation. Fortunately, however, their volume scales more directly with the load current they can supply. To source 10 to 100 mA, the capacitor must be high-valued (1-2  $\mu$ F), and for high voltage rated capacitors this high value is only found in film capacitors. Such capacitors are often 0.5" on a side or larger. If, however, the supply must only source 10s to 100s of  $\mu$ A, the capacitor can be much smaller—high voltage 10-50 nF capacitors can be found in small, surface-mount ceramic packages.

PowerBlade eschews energy harvesters and transformers, due to scaling challenges, and instead embraces a capacitor-fed, Zener-regulated power supply. The key to making this design point viable is scaling the electronics power draw down to meet the limited supply.

## 2.2 Voltage Measurement

A true power meter must acquire time-synchronized voltage and current measurements and multiply them together to obtain power. The voltage channel is frequently obtained by intercepting the plug’s prongs and using a voltage divider to obtain a scaled-down version of the voltage signal [3, 6, 17, 26]. Unfortunately, intercepting the power lines to obtain the voltage is not possible in a planar design. Other designs distribute the voltage and current measurements, and wirelessly recombine them, to obtain power [20, 28], while others do not use the voltage channel signal at all [23]. None of these approaches are ideal for a plug-through meter. Taking distributed measurements requires at least two different devices which increases cost and makes deployment cumbersome, while only using the current channel leads to errors for non-unity power factors [20].

In contrast with the prior work, PowerBlade borrows an idea from the FlipIt plug-through USB charger [22] for its voltage acquisition. FlipIt uses spring-loaded wire contacts molded into a 0.066” thick piece of plastic through which a plug’s prongs pass. PowerBlade improves upon this design by integrating the contacts directly into the PCB by employing a rigid-flex material which eliminates the molding, enabling the only meter design point that makes contact with the prongs without the need for an AC receptacle.

## 2.3 Current Measurement

Among the meters we survey, the most common methods for measuring current employ a sense resistor placed in series with the electrical path [3, 6, 17, 26], a Hall effect sensor placed co-planar to a current carrying conductor trace [26], and a current transformer (CT) that encircles the current carrying conductor [20, 23]. Unfortunately, none of these designs are suited to an essentially planar, plug-through form factor. Current sense resistors are inexpensive, accurate, and small, but they require the electrical path to be broken and an AC receptacle and prongs be used, making them unsuitable for our application. Hall effect sensors work by measuring the deflection of electrons in a conductor exposed to a magnetic field (like the one generated by a current). However, they require the magnetic field lines to be perpendicular to the plane of the sensing element which, in our case, is challenging since the magnetic field lines are co-planar with the circuit board; hence a Hall effect sensor would require a non-trivial third dimension.

In contrast with these methods of current sensing, PowerBlade uses an optimally-placed surface mount inductor to measure the variation in magnetic flux produced by a current carrying conductor, detectable as a voltage across the inductor’s terminals. Used in this way, the inductor functions as a search coil (or inductive sensor) whose terminal voltage is proportional to the rate of change of the current over time. This approach requires signal integration to recover the original current signal. Using a small, surface mount inductor in this manner enables PowerBlade to maintain an essentially two-dimensional form factor—something that is difficult using conventional current sensing methods.

## 2.4 Power Calculation

There exist three common options for calculating power. The first is to use a power metering integrated circuit like the Analog Devices ADE7753 [1]. Three of the surveyed meters employ this or a similar chip [3, 17, 26]. These metering chips take as inputs current and voltage signals and provide as outputs real, reactive, and apparent power, as well as power factor, zero crossings, and other measurements. They provide accurate measurements but are costly in terms of area and power draw, consuming 0.3” × 0.3” × 0.08” PCB area and drawing 25 mW, respectively, placing them outside of acceptable area and power budgets for our application.

A second option employed by several meters in our survey is to calculate power from the acquired current and voltage in software running on an embedded microcontroller. This approach can be quite accurate but the accuracy is bounded by the sampling rate of the ADCs and the performance of the signal processing pipeline. PowerBlade employs this approach and uses a low power microcontroller to achieve an acceptably lower power draw.

In contrast with these approaches—hardware and software—the Monjolo design does not report true power [23]. A Monjolo power meter does not actually sample either the current or the voltage waveform. Rather, it uses a fixed  $V_{RMS}$  value and an approximation of the  $I_{RMS}$  value based on the activation interval of an energy harvesting sensor. With these data, Monjolo estimates apparent power, which is the per-cycle product of  $V_{RMS}$  and  $I_{RMS}$ , but not real or reactive power. Moreover, Monjolo exhibits high error for certain loads with significant harmonic content.

## 2.5 Data Communication

To be useful, a power meter must communicate its data to the outside world. How these data are communicated to users affects the meter size. All of the commercial meters we survey communicate their data to the user with an LCD display on the unit [3, 6, 17]. Of these three, the Kill-A-Watt and Watts Up have a readout physically located at the outlet while the Conserve Insight offers a readout on a five foot tether. Although a display improves data visibility, it also couples the size of the meter with the size of the screen, leading to a tension between making the meter smaller and making the screen larger. This tension affects usability as more readable screens take up more space. In addition, data displayed solely on a screen cannot be easily recorded by the user for later use. Thus, LCD screens are not well-suited to the challenge of pervasive power metering.

Another communications option is wired, like USB or Ethernet, and one of the commercial meters we survey uses this method in addition to its LCD readout [17]. Although this offers an attractive low power, high-bandwidth link, the form factor ramifications are severe. The USB connection must be isolated from AC mains to be connected to a host computer, and this isolation requires substantial additional space that is unavailable in an essentially planar design.

Low power wireless radios allow the system to display or process data remotely, using a smartphone or computer. Unlike an LCD, radios require physically very little space in the meter. The radio-enabled meters we survey use 802.15.4, and ACme [26] uses a multi-hop mesh network, allowing data to propagate over potentially long distances. However, none of these meters allow users to connect directly using a smartphone. PowerBlade also employs a radio, but we chose a Bluetooth Low Energy radio which can directly leverage the rich interface available on nearby smartphones and will soon support IP connectivity and end-to-end networking [25].

## 2.6 Alternate Power Metering Methods

Fine-grained power data does not require individual load metering. This analysis explores devices that, similar to PowerBlade, meter consumption at the outlet where power is being drawn, but methods exist for acquiring this data without physical metering. Wu et al. demonstrate the ability to determine appliance on/off state through deployed sensors, and they use preexisting knowledge of the draw of each of these states to determine total power [30]. Further, ElectriSense [24] is able to determine device state simply by monitoring AC voltage at a single point and measuring the EMI generated by switched mode power supplies and propagated by the wiring throughout the building. Both options provide consumption information without the overhead of plug-load meters, but they also require prior knowledge of the systems to be measured.

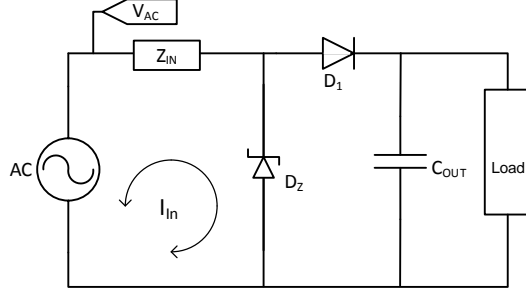


Figure 2: Zener regulated, half-wave rectified power supply.  $Z_{IN}$ , either a resistor or capacitor, is used to shunt the line voltage.  $D_1$  is a rectifying diode.  $C_{OUT}$  is used to store charge between each positive half cycle of the AC wave. The maximum voltage exposed to the load is controlled by the Zener voltage of  $D_Z$ . On very low power loads, this supply can be made in a very small volume.

### 3. DESIGN

PowerBlade performs the same five functions as other power meters, but in a planar, plug-through form factor. This section examines the design space and tradeoffs in achieving this design point.

#### 3.1 Power Supply

PowerBlade optimizes for size by using a power supply design that does not require an IC [21]. Figure 2 shows a Zener regulated, half-wave rectified power supply. This circuit offers a low component count, and only the shunt impedance,  $Z_{IN}$ , must be rated for AC voltage. The choice of  $Z_{IN}$  affects the final system's available power, overall volume, and idle power draw. In this study, we only examine components rated for the application: leads separated by at least the AC mains spark gap of 1.25 mm (package 1206 and larger). Resistors are further rated for the idle power dissipated ( $V_{AC}^2/R$ ), and capacitors must be class X (AC rated "across the line") or above.

We note that this circuit is not isolated. Its ground is tied directly to the neutral line, which could be a possible safety issue when interacting with the circuit. Since the system is wireless, and is intended to be entirely packaged, this does not present a risk for the end user. More discussion on packaging is included in Section 5.2.4. One aspect of safety that does pertain here, however, is component count. In order to limit inrush current if  $Z_{IN}$  is a capacitor, it must be in series with a resistor. Further, when the system is de-powered the capacitor maintains its voltage. In order to prevent shock, an additional high-value bleed resistor must be placed in parallel with the capacitor. If  $Z_{IN}$  is a resistor, neither extra component is required. Although this is not explicitly included in the volume discussion below, it must be considered when selecting the final design.

Figure 3 shows the design space for  $Z_{IN}$  based on component volume and supplied current. A third parameter, not pictured, is idle power: the resistors add an idle power even when the load is not applied. This idle power scales directly with current supplied. Capacitors, however, do not affect idle power. The current draw follows Ohm's law ( $I_{MAX} \approx V_{AC}/Z_{IN}$ ). Volume is calculated using components from DigiKey's electronic component database, and for resistors the smallest available component with the required power rating is shown.

This figure illustrates the fundamental tradeoffs for this simple supply: the volume occupied by the supply scales directly with the provided current. In other words, current is not free even though the system is attached to AC. Whether for resistors or capacitors, accommodating more current means moving to a larger package. Even within a given package, small variations are introduced, while small variations in value result in quantum jumps in volume.

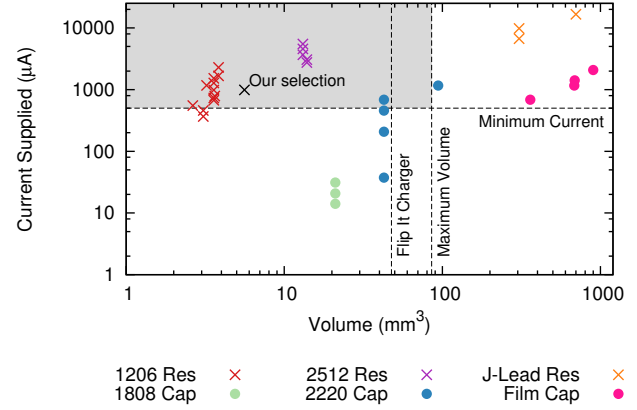


Figure 3: Selecting  $Z_{IN}$  based on volume occupied and current that can be supplied. If  $Z_{IN}$  is a resistor, lower resistance provides more current but also requires a larger size/package to dissipate the additional power. A capacitor does not increase idle power, and high capacitance (low impedance) provides more current but the extra capacitance requires a larger size/package. The resistors marked are the smallest available at the required power rating. There is a maximum volume that the system can occupy, as well as a minimum current required. The upper left quadrant, shaded, represents the viable design space for PowerBlade. Although any component in this quadrant is viable, there exist pareto-optimal points for volume, current, and idle power. We select a 1210 resistor, marked, back from the frontier to allow for tolerance as we develop the design.

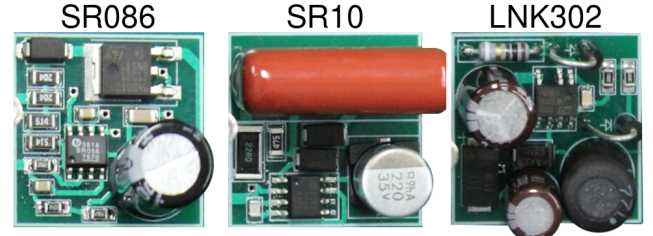


Figure 4: Low volume power supplies. Each supply is built within a 0.875 inch square. Large volume components are necessary for each supply and cannot be reduced significantly as load power decreases.

This relationship holds true for larger systems with increased power requirements. Figure 4 shows three low volume, direct rectification power supplies: the SR086 [13], the SR10 [14], and the LNK302 [9]. Each is dominated by one or more large components whose sizes scale with the current that can be supplied. The relationship is not limited to capacitors and resistors: although the SR10 uses a capacitor shunt similar to PowerBlade, the SR086 and LNK302 use a high-voltage transistor and inductor, respectively. All three of these supplies would exist in the far upper right of Figure 3, providing significantly higher current but requiring greater volume.

Figure 3 can be used to determine an approximate power point for the system. This can be used to select the remainder of the components, which in turn will yield a more precise minimum required current. The maximum volume and minimum current shown on the figure are for the final PowerBlade system. The range of acceptable volumes is determined experimentally on several NEMA outlets, with an additional dashed line representing an approximation of the Flip It USB charger's volume which also utilizes a very similar form factor and usage model.

The upper left quadrant of [Figure 3](#), shaded, is the viable design space for PowerBlade. The pareto-optimal point for current is a 10 k $\Omega$  2512 resistor that can supply 5.5 mA and requires 13.1 mm $^3$ . The pareto-optimal point for volume is a 47 k $\Omega$  1206 resistor that can supply 1.1 mA and requires 3.2 mm $^3$ . These would add an idle power of 1.4 W and 300 mW, respectively. The pareto-optimal point for idle power is a 33 nF 2220 ceramic capacitor that can supply 684  $\mu$ A and requires 42.8 mm $^3$ , but adds no idle power. Our selection is also marked, a 1210 resistor selected away from the frontier to provide ample tolerance in power dissipation and design flexibility as we continue to develop the system. We selected a resistor just over our minimum current threshold to minimize idle power draw.

### 3.2 Voltage Sensing

Voltage sensing in this form factor requires a planar contact method, a voltage divider, and an ADC to acquire the voltage signal digitally. Of these, the method to contact AC voltage is the only requirement that cannot be solved with small, readily available components. We have identified two possibilities for contact: small spring loaded pins and flexible tabs built into the PCB itself.

A flexible tab built into the PCB bends to provide contact as the AC plug is inserted (this is the contact method shown in [Figure 1](#)). The benefit is easy manufacturing: the process of printing the circuit board provides the contact method. The tradeoff is in longevity. The flexible materials are not designed for elasticity, and after several insertions the flexible tab no longer provides a strong contact.

Another option is to mount a spring loaded pin sideways in the plane of the PCB. If the tip of the pin is rounded, the AC plug can slide past it as the spring-loaded pin applies contact. Such components are available off the shelf [10], and since they are designed to be compressed, they will maintain contact over more insertions than flexible tabs. The tradeoff is in the difficulty in manufacturing: mounting the pins is currently a manual procedure. We have yet to identify a process to reliably and repeatably mount the pin.

### 3.3 Current Sensing

Many existing current sensing techniques, like shunt resistors, are planar, but rely on interrupting an AC conductor, which PowerBlade cannot do. Instead, PowerBlade senses current non-intrusively by detecting the magnetic field surrounding an alternating current. As current passes through the AC prongs inserted through PowerBlade, the charge moving through each prong generates a magnetic field. Those fields add constructively between the prongs and destructively outside the prongs. [Figure 5](#), generated by applying the Biot-Savart law, shows the relative strength and orientation of this magnetic field in the plane of PCB surrounding the prongs.

Two aspects of this figure guide the optimal placement of a sensor to measure this field. First, the magnitude of the field is on the order of 10-100 nT, which establishes bounds on the required transducer sensitivity. Second, although intuition might suggest that the constructive fields would be maximized directly between the prongs, the rapid decrease in field strength with distance from the conductor means the strongest signal is closest a prong.

Hall effect sensors and other vector magnetometers are capable of sensing this magnetic field, but packaged units cannot meet PowerBlade's form factor needs or power requirements. Many such devices also fail to meet the requirements of this system's design due to low sensitivity or low sampling rates. Instead, we observe that a surface mount wirewound inductor placed in the field can act as an inductive sensor or magnetometer. The alternating current in the wire causes a changing magnetic field which passes through the coils of the inductor and generates a voltage. A coil magnetometer used in this way is also known as a search coil [29].

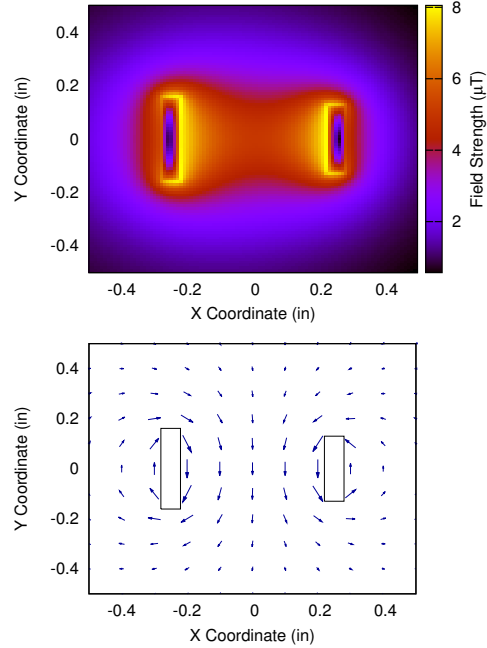


[Figure 5](#): Superposition of magnetic fields around the prongs of an AC load plugged through PowerBlade. The top figure shows the relative magnitude of the field and the bottom shows the direction and relative magnitude, both with a 1 A constant current. The current flows in opposite directions in the prongs, so the fields add constructively between the prongs and destructively outside. Between the prongs, the field is largely oriented vertically. This model allows us to optimally position and orient a wirewound inductor in the field to maximize induced voltage.

$$V = -\mu N A \frac{dH}{dt} \quad (1)$$

The equation governing the voltage generated in the coil can be determined from Faraday's law of induction and is shown in [Equation \(1\)](#), where  $\mu$  is the magnetic permeability,  $N$  is the number of turns in the coil, and  $A$  is the cross-sectional area of the coil. Note that voltage is proportional to the change in magnetic field strength over time. This means that voltage on the inductor is proportional to the change in current over time, rather than the current itself. The signal must be integrated to recover the original current waveform.

### 3.4 Power Calculation

If the form factor or power requirements prevent the use of a dedicated metering chip, as is the case for PowerBlade, then the only remaining option is to implement custom measurement software in a low power microcontroller. However, the choice of microcontroller must balance the fidelity of measurements with the availability of power. For example, a higher sampling rate will improve measurement accuracy, but it will also draw more power due to increased data conversion rate and more frequent processor wakeups. Similarly, the measurements themselves must be scaled from raw "ADC counts" to power statistics (W, VA, etc.) through various transfer functions that may require floating point arithmetic. The floating point operations could be performed on the PowerBlade unit itself, power and performance permitting, or they may be applied in the receiver. The particular operating point depends on a balance of many variables.

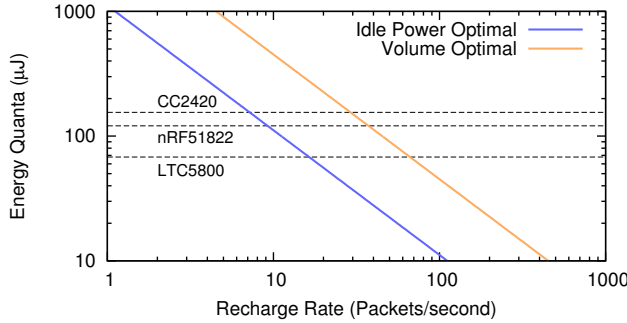


Figure 6: Maximum energy quanta vs recharge rate for two options for  $Z_{IN}$ .  $V_Z$  is fixed at 10 V. Both optimal volume and optimal idle power draw are shown, and increasing  $C_{OUT}$  results in a higher energy quanta at a slower recharge rate (upper left corner). The minimum energy to boot and send a packet is shown for three radio transceivers. For a given  $Z_{IN}$ , the maximum packet transmission rate for each transceiver lies at the intersection of the dotted line with the given curve.

### 3.5 Data Communication

Data communication often requires a continuous burst of power. For a wireless radio, this is the energy required to send a single packet, but even a display screen must display for a minimum duration to allow a human to read it. In some cases, the current required may be more than what is available, and if so, the power supply must store at least the energy required for a single such event (referred to here as energy quanta). How much energy is available is determined by three components from Figure 2:  $Z_{IN}$ ,  $V_Z$ , and  $C_{OUT}$ .

Increasing  $C_{OUT}$  will increase the energy available, but at the expense of a slower recharge rate. Decreasing  $Z_{IN}$  results in greater current supply, which will increase both recharge rate and energy quanta (as additional current is available during the discharge event). Increasing  $V_Z$  will increase both energy quanta and recharge time, but will increase energy quanta more due to the quadratic term in energy calculation. Higher  $V_Z$  values are therefore preferred, but  $V_Z$  is also constrained by other components. Small options for  $C_{OUT}$  are commonly limited to 16 V, and many of the commercially available miniature buck converters offer significantly higher efficiencies in the 10-15 V range.

Figure 6 shows the recharge rate and energy quanta for two of the three pareto-optimal options for  $Z_{IN}$  from Section 3.1. The current optimal option is not shown; it could supply sufficient current to continuously operate certain radios but is undesirable due to its high idle power draw.  $V_Z$  is fixed at 10 V, and for a given curve, increasing  $C_{OUT}$  results in moving up and to the left. The range of capacitance shown for each curve (up to 22  $\mu$ F) is readily available in a variety of small ceramic packages.

Also shown is the minimum energy required to boot and send a packet for three possible radios, the CC2420 [15], LTC5800 [8], and nRF51822 [11]. The measurement of the CC2420 was performed by Yerva et al. [31], the figure for the LTC5800 is available in its datasheet, and we measure the energy for the nRF51822 ourselves. The energy quanta figures need not be exact; their purpose is to drive the selection of a radio.

For a given radio and selection of  $Z_{IN}$ , the maximum recharge rate, in packets per second, is the intersection of the two lines. This can be used to determine the possible data rate or, if the required recharge rate is lower,  $Z_{IN}$  can be reduced from the optimal to reduce idle power. The latter is the case in PowerBlade.

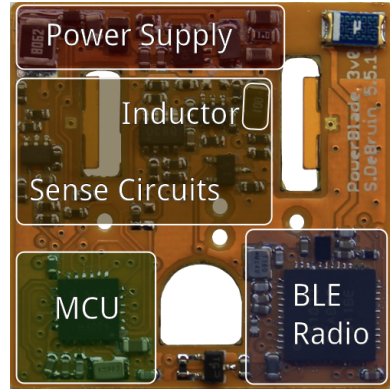


Figure 7: PowerBlade PCB layout with key features labeled. Exact board dimensions are 1"  $\times$  1"  $\times$  0.066". The position of the sense inductor, placed close to the neutral prong, is marked.

$Z_{IN}$ (Z)	Expected	Actual	Volume	Cost	Idle Power
22 nF (120 k $\Omega$ )	456 $\mu$ A	451 $\mu$ A	43.0 mm $^3$	\$1.24	0 mW
33 nF (80 k $\Omega$ )	705 $\mu$ A	740 $\mu$ A	43.0 mm $^3$	\$1.63	0 mW
56 nF (47 k $\Omega$ )	1161 $\mu$ A	1137 $\mu$ A	95.0 mm $^3$	\$1.34	0 mW
100 k $\Omega$	550 $\mu$ A	538 $\mu$ A	2.6 mm $^3$	\$0.03	140 mW
80.6 k $\Omega$	687 $\mu$ A	658 $\mu$ A	3.0 mm $^3$	\$0.03	170 mW
75 k $\Omega$	733 $\mu$ A	716 $\mu$ A	3.0 mm $^3$	\$0.03	190 mW

Table 2: Expected and actual maximum current for various possible component choices for  $Z_{IN}$  in the supply in Figure 2. Also shown are the volume required and cost of each component, as well as its idle power draw when the system is connected to AC.

## 4. IMPLEMENTATION

This section describes how the components identified in Section 3 are integrated into a system in PowerBlade. This section also covers the steps required to operate the system as a true power meter, including how the wireless system is used and how the meter is calibrated.

### 4.1 Power Supply

We explore several components for  $Z_{IN}$  to evaluate their performance. Table 2 shows the expected maximum current from the supply and our experimentally measured actual current, as well as the volume, cost, and idle power that result from that component being selected. Resistors are able to deliver comparable current to that of capacitor shunts for a smaller volume and lower cost, but they increase idle power draw even when the load is powered off.

Although early versions of PowerBlade had footprints for both a 2220 package capacitor and 1210 package resistor, current designs optimize for size and cost by only providing space for the resistor. In addition to the significantly smaller size, the low cost of a resistor outweighs the cost added by its idle power. At \$0.12 per kilowatt-hour, the 170 mW added by an 80 k $\Omega$  resistor would outweigh the cost of a 33 nF capacitor only after nine years of continuous operation. Current implementations use an 80.6 k $\Omega$  resistor, which leads to a design constraint for the rest of the system in that it must operate below a maximum average current of about 658  $\mu$ A. Summing the power draw of the system and the idle power draw of the supply, this leads to an overall power draw of 176 mW for PowerBlade. Our present choices reflect the desire for frequent data transmissions supporting interactive use, but we note that higher  $Z_{IN}$  values are also possible with a concomitant reduction in data transmission rate.

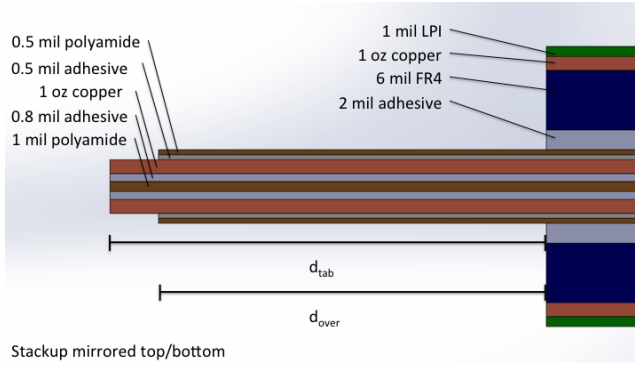


Figure 8: Cross-sectional layer stack-up in PowerBlade. Shown are the entire stack-up (right), as well as the stack-up of the tab itself (left) that contacts the AC plug. Using a rigid-flex PCB allows for easy manufacturing with multiple insertions.

The remainder of the components from Figure 2 are a 10 V Zener diode and 250 mA rectifier diode, both in a small SC-79 package, and a combined 55  $\mu\text{F}$  from two parallel capacitors for  $C_{OUT}$ . We select a larger capacitance than the minimum required from Figure 6 to allow tolerance as we continue the design, and the added delay is only experienced when the unit is first powering on. The load will nominally see 8.9 V: the Zener voltage minus the rectifier forward voltage of 1.1 V. To regulate this output to 3.3 V we use a 3.3 V buck regulator, the Texas Instruments TPS62122 [16]. At the nominal input voltage of 8.9 V this regulator has an efficiency of 85-90%.

## 4.2 Contact

The single-PCB system shown in Figure 1 is a rigid-flex PCB—a stack-up of layers of both rigid and flexible materials with conductive copper layers sandwiched in between. For our proof of concept we select flexible tabs over spring loaded pins due to the ease in manufacturing. This method of circuit board construction maintains good contact for approximately 10-30 insertions, providing a pathway to a proof of concept, but we intend to continue to explore methods using spring loaded pins in future work.

Figure 8 shows a cross section of the flexible tabs. The innermost layers of the PCB are all flexible, the inner layers 2 and 3 of copper are fixed to a flexible polyimide core. These layers extend into the tabs to make contact with AC. They continue throughout the entire system, but are rigidized with FR4 material between this flexible core and the outer copper layers.

Extending only 5 layers into the tab provides insufficient support; the tabs bend on the first insertion and never return to form. Instead, we add an additional polyimide/adhesive pair on each side of the tab, with only the tip remaining exposed for contact. After exploring several options for  $d_{over}$ , we find that fully covering one side of the tab while exposing only the tip on the other side allows for maximum insertions. This requires loads be plugged through PowerBlade from back to front, but NEMA polarization means most loads already plug from this direction.

## 4.3 Measurement Amplifiers

Figure 9 shows the amplifier circuits used to measure voltage and current. PowerBlade measures line voltage directly through a voltage divider with a  $V_{CC}/2$  offset to measure both positive and negative phases.  $R_F = 4.99 \text{ k}\Omega$  and  $R_{I1} = R_{I2} = 953 \text{ k}\Omega$ , so  $V_{SENSE}$  can be approximated as Equation (2).

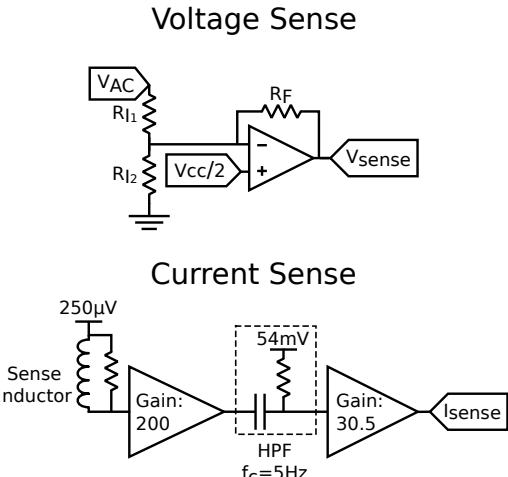


Figure 9: Voltage and current sensing circuits. Voltage sensing requires little volume, consisting of a voltage divider and amplifier with a  $V_{CC}/2$  offset. Current sensing uses a horizontally wirewound inductor, amplified and filtered. The resulting signals  $V_{SENSE}$  and  $I_{SENSE}$  are measured by the MSP430.

$$V_{SENSE} \approx \frac{V_{CC}}{2} - 5.24 \times 10^{-3} V_{AC} \quad (2)$$

Based on these configurations, the voltage signal has a peak to peak amplitude of 1.79 V where the AC is 120  $V_{RMS}$  (United States) and 3.28 V where the AC is 220  $V_{RMS}$  (much of Europe and China).

PowerBlade measures the signal from the sense inductor in multiple stages. The inductor is referenced to 250  $\mu\text{V}$  and amplified in two stages with a combined gain of about 6100x. Low frequency noise is removed with a high pass filter between the first and second stages, and this filter is referenced to 54 mV so the final signal is centered around  $V_{CC}/2$ .

$$I_{SENSE} \approx \frac{V_{CC}}{2} + \alpha \frac{dI}{dt} \quad (3)$$

Equation (3) describes the output of the current sense stage as a function of the derivative of the AC current, where  $\alpha$  is a lumped parameter consisting of the characteristics of the coil, gain, signal distortions, and general uncertainty. After integration the current is represented by Equation (4), where  $\beta$  accounts for DC offsets in the system and integration offsets.

$$\text{Current} \approx \int \left( \frac{V_{CC}}{2} + \alpha \frac{dI}{dt} \right) dt \approx \alpha I + \beta \quad (4)$$

## 4.4 Calibrating PowerBlade

PowerBlade calibration requires two steps. The first step is to measure the scaling and offset values  $\alpha$  and  $\beta$ , which must be done once per design. The second step is a device-specific calibration that accounts for slight variations between units.

To determine the scaling and offset values  $\alpha$  and  $\beta$ , respectively, we measure the reported RMS current from PowerBlade for a range of resistive (unity power factor) loads. Figure 10 shows the RMS values of current reported as raw values. For the current system, these measurements are linear with an  $R^2$  value of 0.999, and indicate an  $\alpha$  of 40.85 and  $\beta$  of 25.0. Subtracting the offset  $\beta$  happens in PowerBlade, and for further testing, all units comprising a batch are programmed with this value.

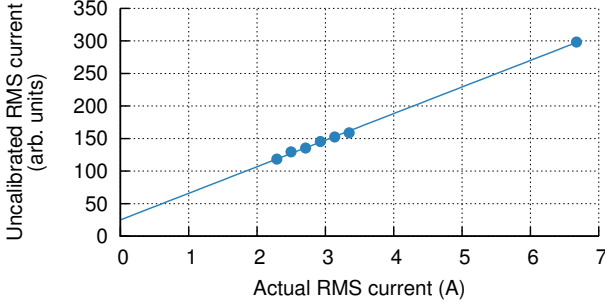


Figure 10: PowerBlade reported uncalibrated RMS current. These samples are used to calculate  $\alpha$  and  $\beta$  from [Equation \(4\)](#) and allow us to refine our power calculations.

To reduce the computational burden on PowerBlade, we divide by  $\alpha$  in the receiver, and for increased accuracy, each unit is calibrated again. We connect each PowerBlade in a batch to a 200 W load to compute a device-specific  $\alpha$ , store that value in FRAM, and transmit it with each packet. We have observed a mean value for  $\alpha$  across multiple units of 41.79, with a 95% confidence interval of 1.87.

Finally, after calibrating  $\alpha$  for each device, we notice an exponential error not accounted for by the model. We experimentally determine the following correction  $P = P_{RAW} - 6.6e^{-0.015P_{RAW}}$ , where  $P_{RAW}$  is the power (in watts) after applying the  $\alpha$  and  $\beta$  corrections, removes this error and yields the final power figures. The values of 6.6 and -0.015 are determined once per design.

## 4.5 Power Calculation

We save the overhead of a power metering IC by performing our power metering calculations on a MSP430FR5738. This chip is the master controller of the system and is the only component not automatically power gated at startup. It is selected due to its small size, power efficiency of 81.4  $\mu$ A/MHz, and integrated 16 kB non-volatile FRAM, eliminating an external component.

To measure power, the MSP430 samples  $V_{SENSE}$  and  $I_{SENSE}$  at 2.52 kHz (42 samples per AC cycle). This frequency is both an even divisor of our timing clock (32,768 Hz) and an even multiple of the frequency to be sampled (60 Hz). Because  $I_{SENSE}$  is proportional to the derivative of current, the second measurement step integrates  $I_{SENSE}$  to obtain current ( $V_{SENSE}$  is a good representation of voltage). The integration is performed in software, but could be performed by hardware in the future. The final calculation step involves calculating power from voltage and current.

Because the MSP430 has real-time access to both voltage and current waveforms, it can function as a true power meter. Real power is determined by multiplying voltage and current at each point, and then averaging over the number of samples. Apparent power is determined by first calculating the root mean square voltage and current over a cycle,  $V_{RMS}$  and  $I_{RMS}$ , respectively, and then multiplying them. Knowledge of both real and apparent power allows the system to determine reactive power as well as the power factor of the load. Real power is also aggregated in the MSP430 to compute total watt-hours measured over time, and this number is stored in FRAM.

## 4.6 BLE Communication

Data are transmitted in broadcast-style BLE advertisement messages. The MSP430 first communicates to the nRF51822 via UART at 38,400 baud, and the nRF51822 repeats this data in the advertisement. The MSP430 sends UART data nominally at 1 Hz, and the nRF51822 sends advertisements at 5 Hz, so 4-5 identical packets are transmitted each second. This greatly increases the likelihood of

reception, and does not dramatically affect the power draw.

In addition to a sequence identifier and information regarding versioning and scaling, each PowerBlade packet contains four fields: line voltage, instantaneous real power, instantaneous apparent power, and watt-hours. Real power and apparent power are 1-second averages, and can be used together to calculate power factor. Watt-hours is an over-time total, and in the event of zero packet loss watt-hours will, once scaled, also equal the integral of real power.

PowerBlade is robust against packet loss. The intended recipient of broadcast advertisements is either a smartphone or a fixed BLE receiver, but in the event of no receiver, only the resolution of the missed packet is lost. The overall watt-hours total remains an accurate reading in any received packet. Watt-hours is stored as a 32-bit number and can overflow. In the worst case with present calibration scaling values, measuring an 1,800 W load will lead to an overflow every 29 days. A 100 W load will overflow after 523 days of continuous measurement. Overflows are signaled in the advertisements so the true watt-hours reading can be recovered. If a receiver is not present for long periods of time, potential for data loss exists.

## 4.7 System Operation

[Figure 11](#) shows the startup phase of PowerBlade and 7 s of steady-state operation. When the system first starts, there is only power to boot the MSP430; if more components are drawing power, the 3.3 V power rail will never enable and the system will lock up. Instead, MOSFETs separately power gate the sensing circuits and BLE radio. With only the MSP430 running, the capacitor charges, enables the 3.3 V rail, and eventually reaches a nominal 8.9 V.

When the MSP430 detects that the capacitor has charged to the nominal voltage it enables the sensing circuits, and these remain powered for as long as PowerBlade is powered. The MSP430 spends 1 s collecting measurements before enabling the nRF51822, which also remains powered for the duration of the trace. At this point the device has entered steady-state operation.

## 5. EVALUATION

We evaluate PowerBlade on the basis of accuracy in reporting real power for both a calibrated resistive AC load and an assortment of household loads. We also present benchmarks that affect the usability of the system, including PowerBlade’s volume, cost, wireless performance, and safety of using the system.

### 5.1 Power Metering Accuracy

We evaluate PowerBlade’s accuracy in two parts. First, we explore bench top accuracy, where we use PowerBlade to measure the power draw of a programmable AC load—the APS 3B012-12 [2]—set to unity power factor. This allows us to measure a large part of the metering range (up to 1200 W) in defined increments and in a controlled setting. Second, we use PowerBlade to measure the power draw of several household items. Although not an exhaustive list, this is representative of PowerBlade’s target usage.

For the bench top accuracy, ground truth is provided by the 3B012-12 itself via its serial interface. For the household tests, ground truth is taken from two sources. On the low range, we use a professionally calibrated Power Line Meter (PLM) [5]. This device is limited to 480 W, however, so to measure larger loads we take ground truth from a Watts Up [17]. We report the Watts Up measurements over the low range as well, and it is clear that it is less accurate than the PLM (typical error of about 1.72%). The need to use two different meters for ground truth demonstrates the difficulty in creating a highly accurate whole-range metering solution. For each test we take 30 PowerBlade measurements, 30 ground truth measurements, and report the arithmetic mean and 95% confidence interval.

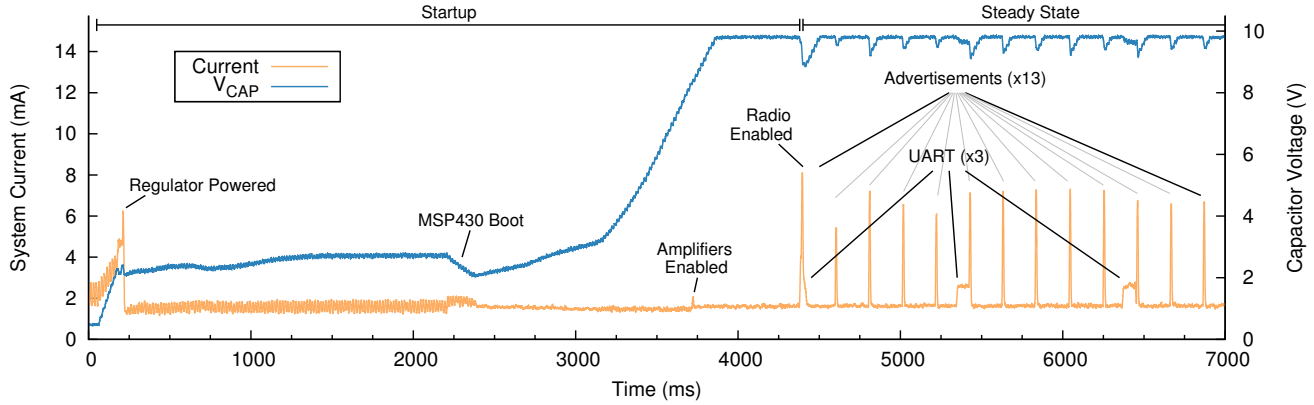


Figure 11: PowerBlade timing: storage capacitor voltage and 3.3 V regulator output current for the first 7 s of operation. At startup the measurement circuits and the nRF51822 are automatically disabled. For approximately 2 s the capacitors charge gradually, and around 2.25 s the MSP430 boots. When the MSP430 detects the capacitor has charged to the nominal voltage of 8.9 V it enables the voltage and current measurement circuits. For the first 1 s of the amplifiers being powered there is no data to transmit, so the nRF51822 is kept disabled. After 1 s of measurement the MSP430 enables the nRF51822 and sends data over UART. At this point the nRF51822 begins advertising data at 5 Hz for the remainder of operation and the MSP430 updates with new information over UART at 1 Hz. This results in up to five identical packets transmitted, which increases the likelihood of reception, and a sequence number transmitted with each packet denotes the duplicate.

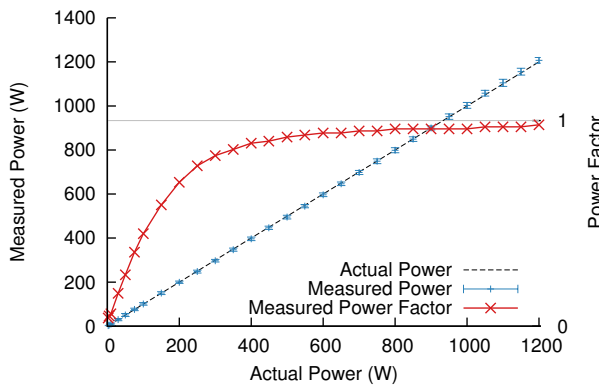


Figure 12: Metering accuracy for a variable resistive (power factor equals 1) load: measured power vs actual power as well as measured power factor. Also shown are the 95% confidence intervals for real power. The minimum AC load for accurate metering is about 2 W and over the range from 2 W to 1200 W the average accuracy in real power is 1.13%. PowerBlade’s metering and reporting system is accurate over a range of resistive loads.

### 5.1.1 Resistive Loads

Resistive loads with a unity power factor, which include incandescent lights and power-factor-corrected devices, exhibit a sinusoidal current waveform in-phase with voltage. To measure PowerBlade’s accuracy in this simple but common case, we use an APS 3B012-12 programmable AC load set to a fixed unity power factor. Figure 12 shows the end-to-end accuracy for PowerBlade metering this resistive load. Displayed are the reported real power and power factor from PowerBlade, as well as the ground truth power up to the programmable load’s maximum of 1200 W. Note that the true power factor is equal to one throughout the test.

We measure 29 wattages from 2.2 W to 1200 W: 50 W to 1200 W in increments of 50 as well as 2.2 W, 5 W, 10 W, and 75 W. For these measurements the average error is 2.3 W and the average percent error is 1.13%. At 2.2 W the error is 0.21 W (9.5%) and at 1200 W the error is 7.01 W (0.6%).

Device	PF	Power	Watts Up Error	PowerBlade Error
150 W Bulb	1.00	162.17 W	1.22 W (0.75%)	-0.99 W (0.61%)
Fridge	1.00	108.22 W	—	-5.30 W (4.90%)
Drill (Max)	0.99	235.21 W	1.69 W (0.72%)	2.96 W (1.26%)
Toaster	0.99	827.87 W	—	-22.11 W (2.67%)
Vacuum	0.98	1246.96 W	—	15.24 W (1.22%)
Microwave	0.92	1729.73 W	—	16.01 W (0.93%)
Hot Air	0.83	305.54 W	0.88 W (0.29%)	-1.93 W (0.63%)
TV (Normal)	0.62	196.23 W	0.86 W (0.44%)	-9.03 W (4.60%)
50 W CFL	0.61	48.57 W	-1.08 W (2.22%)	-9.51 W (19.58%)
TV (Static Image)	0.61	129.51 W	-0.04 W (0.03%)	-4.00 W (3.09%)
Xbox	0.57	50.44 W	0.64 W (1.27%)	-0.83 W (1.65%)
MacBook	0.51	52.68 W	-0.41 W (0.78%)	-4.49 W (8.52%)
Blender	0.49	106.63 W	1.95 W (1.83%)	36.97 W (34.67%)
Router	0.46	9.11 W	0.22 W (2.41%)	-0.62 W (6.81%)
Drill (Low)	0.30	51.10 W	4.18 W (8.18%)	20.40 W (39.92%)

Table 3: Metering accuracy for a cross section of household devices. On this selection, the average percent error in real power is 6.5%. Although these devices produce more complex waveforms than a fully resistive load, PowerBlade remains acceptably accurate.

### 5.1.2 Household Devices

Resistive loads constitute a large fraction of household devices, but not all loads have sinusoidal current waveforms. Table 3 shows PowerBlade’s accuracy for several devices found in a common household. For these devices, we simultaneously take a PowerBlade measurement, a Watts Up measurement and, if the load is below 480 W, a PLM measurement. If available, the PLM is used as ground truth. If not, the Watts Up is used. Although the fridge draws about 100 W, its start-up power tripped the 4 A fuse in the PLM, preventing PLM measurements for that load. For each device, we report its power and power factor, as well as PowerBlade’s error and, if not used as ground truth, the Watts Up error for comparison.

This set of devices has a range of power from 9 W to 1730 W and a range of power factors from 0.30 to 1. The average absolute error for PowerBlade measurements of these devices is 10 W (4.3x higher than the resistive load), and the average percent error is 6.5% (5.8x higher). This error is dominated by two devices with highly inductive (low power factor) draws: the blender (PF=0.49) and the drill set

to low power (PF=0.30). Each of these devices has an error of over 20 W and a percent error of over 30%, and excluding these two, the average absolute error drops to 7.2 W (3.1x the resistive load) and the average percent error drops to 4.3% (3.8x the resistive load). Correctly metering such devices is an area of future development.

The difficulty in measuring highly inductive loads, and further the difference in accuracy between the programmable load and the household devices, can be partially explained by examining the current waveforms. [Figure 13](#) visualizes the current measurement process in PowerBlade for a few loads from [Table 3](#). The known current signal, measured by a commercial current transformer [7], is shown along with  $I_{SENSE}$ , the signal output from PowerBlade’s current amplifier (which, as described in [Section 3.3](#), represents the derivative of the current waveform). Also shown is the post-integration representation of current. Voltage for each load is synchronized, and zero crossings of the common voltage are denoted by vertical lines.

Visible on the figure is the integral/derivative relationship between  $I_{SENSE}$  and known current, as well as the fidelity of the integrated signal to that known current. For devices with sinusoidal or otherwise smooth current waveforms, the integrated signal tracks well with known current. For other devices, however, high frequency components in the current waveform are suppressed by the integrator, resulting in increased error.

### 5.1.3 Watt-hour Accuracy

PowerBlade is designed to measure and report both instantaneous power and watt-hours, the sum over time that will be used by the util-

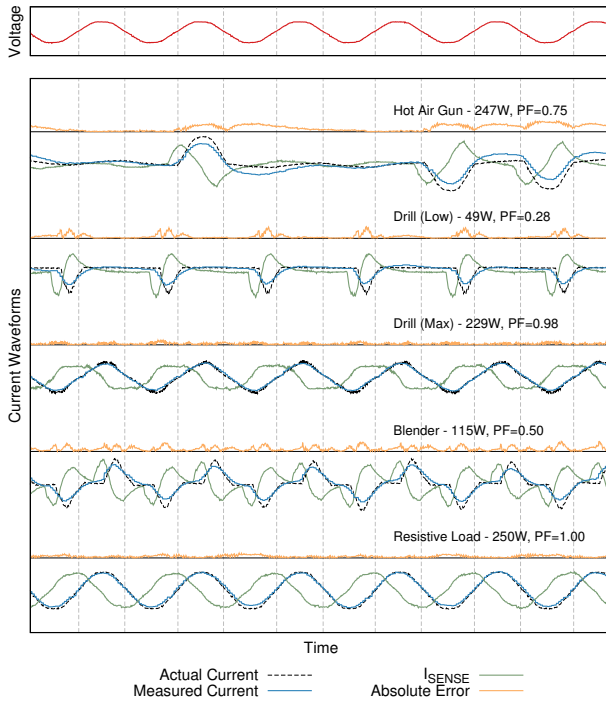


[Figure 13](#): Current sensing fidelity. Output of current sense amplifier,  $I_{SENSE}$ , along with the internal representation of current, are shown for several household devices. Also shown is the true current waveform as measured by a commercial current transformer [7]. Visible is the derivative relationship between actual current and  $I_{SENSE}$ , as well as the distortions introduced by this sensing and integrating technique. This shows that PowerBlade’s current sensing method reasonably captures the current waveform.

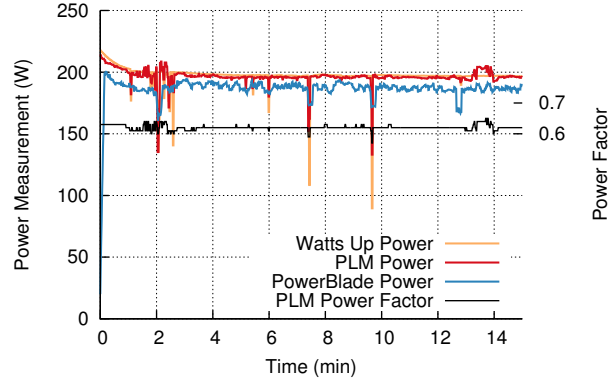


[Figure 14](#): Metering accuracy over time for a television in use. Shown on the figure are reported power from the PLM (ground truth), Watts Up, and PowerBlade, as well as power factor reported from the PLM. At the end of 15 minutes the PLM reported 49.07 Wh, the WattsUp 49.28 Wh (0.42% error), and PowerBlade 46.80 Wh (4.62% error). This is consistent with PowerBlade’s instantaneous error of 4.60% for the television in full use.

ity company to levy charges. The figure of watt-hours also accounts for the possibility that one or multiple packets are not received: resolution is lost but watt-hours remains an accurate long-term measure. To evaluate PowerBlade’s accuracy in reporting watt-hours, we take simultaneous measurements from the PLM, Watts Up, and PowerBlade for a television in normal viewing use. [Figure 14](#) shows the measurements over time from Watts Up and PowerBlade as compared to the PLM.

After 15 minutes of normal television use, the PLM reported 49.07 Wh, the Watts Up reported 49.28 Wh (0.42% error), and PowerBlade reported 46.80 Wh (4.62% error). In instantaneous measurement trials the PowerBlade measurements for the television in full use were off by an average of 4.60%, the watt-hours figure of 4.62% error is consistent with the instantaneous readings.

## 5.2 Usability Benchmarks

PowerBlade’s accuracy makes it comparable to other power metering systems, but it is the usability of the system, and in particular the size, cost, and wireless communications, that most distinguish it. We also show through standard safety testing that PowerBlade is safe to use with the addition of an enclosure.

### 5.2.1 Volume

The defining characteristic of PowerBlade is its volume: the entire system is a single PCB. This circuit board is 1.0" on a side, and the PCB itself is 0.023" thick. The thickest component on the surface is the antenna at 0.043", so the combined total thickness of the system is 0.066". This is the same thickness as the pass-through section of the FlipIt charger, which is a certified commercial product.

### 5.2.2 Cost

The component breakdown in PowerBlade with costs is listed in [Table 4](#). Prior to consumer use, PowerBlade needs an enclosure, but the system could be largely assembled for \$10-\$15 per unit. Although it is important to note the distinction between the cost of PowerBlade and the price of other systems, this is slightly less than the price of Kill-A-Watt (\$23.99) and significantly less than the price of Watts Up (\$130.95). The cost of \$10-\$15 for PowerBlade is also an un-optimized reporting of DigiKey pricing; the minimum viable cost would likely be much lower.

Component	Cost	Component	Cost
MSP430FR5738	\$1.71	Sense inductor	\$0.30
nRF51822	\$1.66	Amplifiers	\$2.51
Antenna, balun, & crystals	\$1.70	MOSFETs	\$0.12
Buck converter	\$0.65	Other passives	\$0.93
		PCB	\$1.47
		Total	\$11.05

Table 4: Cost for the PowerBlade system. The total system is roughly \$11 in quantities of 1,000. We believe this represents an acceptable price point for effective plug-load metering deployments.

### 5.2.3 Wireless Range

We test the effectiveness of PowerBlade communications by measuring packet reception rates in three configurations of PowerBlade units. First we deploy and evaluate a single PowerBlade as a baseline. Next we place three PowerBlade units throughout a room as a more typical deployment case. Finally, we place three units on a single power strip and activate them simultaneously to test for possible packet collisions. We record both unique and total packets received per second. PowerBlade updates data at 1 Hz, and BLE packets are sent at 5 Hz, so nominally we should receive 1 unique and 5 total packets per second.

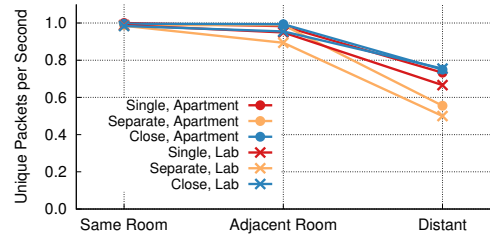
For each configuration we evaluate packet reception rate at three transmission distances, and perform the entire experiment both in an apartment and in a lab. The apartment consists of three rooms, with measurements taken in the same room, adjacent room, and two rooms away. Only a single other BLE device is active in the apartment. The lab consists of one room and hallways, and measurements are taken in the same room, immediately outside of the room in the hallway, and 20 m down the hallway from the room. The lab environment includes 16 non-PowerBlade BLE devices as well as numerous other devices active in the 2.4 GHz band.

Figure 15 shows the reception rate for each of these trials. In all cases, the unique reception rate is at or close to the nominal of 1 per second when in the same or adjacent rooms, but the total reception rate decreases from the same to the adjacent room. Further, the total reception rate is higher in the apartment than in the lab for both distances. Taken together these three results suggest that range and interference do effect BLE transmissions, but the redundancy in PowerBlade helps ensure reliable data communication.

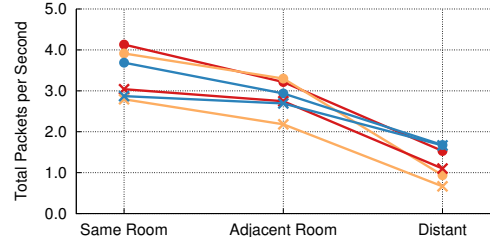
The distant measurements show continued decline in total packets, but also a decrease in unique packets: 20% to 50% of the unique packets are not received at all (all five redundant packets were all dropped). This indicates that this distance—whether two rooms separated in a residential setting or 20 m down a hallway in a university building—exceeds PowerBlade’s usable range. We note that RF designs require some degree of lumped-parameter tuning to achieve maximum performance but PowerBlade’s RF circuitry has not been tuned yet, so that may help explain these results.

### 5.2.4 Safety

PowerBlade is a prototype not designed for consumer use in its current form, but safety when using and deploying the system is still important. The UL safety standard that covers PowerBlade is UL 2735: Standard for Safety in Electric Utility Meters [18]. Although we do not have the resources at this time to perform an exhaustive safety evaluation, the enclosure requirements and single fault and mechanical tests in UL 2735 are good initial benchmarks for exploring the overall safety of the system.



(a) Unique packets received per second



(b) Total packets received per second

Figure 15: Wireless reception rate for PowerBlade. Unique packets per second as well as total packets per second are recorded for each test. PowerBlade units are deployed singly, throughout a room, and adjacent on a power strip. The lab environment includes many other background sources of 2.4 GHz communications which may interfere with PowerBlade broadcasts. When in the same room as or adjacent room to a PowerBlade deployment, advertised power data is received once per second with a high probability.

The primary safety requirement is preventing electric shock by the unit. Figure 16 shows a PowerBlade unit after coating in a resistive material that protects the user from live parts. The resistive material does not noticeably affect wireless performance, and increases the total volume to 0.074 in<sup>3</sup> (12% increase). This currently requires a labor intensive application process, but for future builds we have identified a supplier capable of adding a heat-resistant overmolding in a scalable manufacturing process.

In addition to applying the conformal coating, we evaluate the system based on two sets of safety tests from UL 2735. The first is single fault testing for the electrical system, to determine if a failure in any one component could result in unsafe conditions. We identify three components that, in the event of a fault, will overload other components. In the power supply,  $Z_{IN}$  failing closed (short circuit) will expose the system to increased current, and  $D_Z$  failing open will no longer limit  $V_{CAP}$  to 9 V. In the voltage measurement circuit,  $R_{I1}$  failing closed (short circuit) will expose multiple components to 120 V. Circuit analysis indicates that  $Z_{IN}$  and  $R_{I1}$  failing open will result in no connection (no testing required).  $D_Z$  failing short will simply prevent charging, although we do test this condition.

As expected, shorting either  $Z_{IN}$  or  $R_{I1}$  results in secondary faults in other components. Shorting  $Z_{IN}$  results in open circuit faults in both  $D_1$  and  $D_Z$  ( $D_1$  is visibly damaged) but after 30 minutes there is no detectable change in temperature in the unit. Shorting  $R_{I1}$  results in open circuit faults and visible damage in both  $R_F$  and the voltage measurement amplifier. This test also results in a bright spark, audible pop, and momentary increase in temperature (to 33 degrees Celsius), but the temperature quickly decreases, and after 30 minutes there is no detectable ongoing change. Opening  $D_Z$  results in increasing  $V_{CAP}$  to 23 V, but the 3.3 V regulator continues to operate as normal and the system continues to function. Shorting  $D_Z$  results in no charging, but also no unsafe conditions.



Figure 16: Conformally coated PowerBlade. Shown are the unit after conformal coating has been applied, as well as the conformally coated unit attached to a load. Although this method requires a manual application process that is not manufacturable in large scale, it does protect the user from live parts. In the future an overmolding process will provide similar protection in a manufacturable way.

The second set of tests from UL 2735 is mechanical, to determine if the protective coating in Figure 16 can withstand real world conditions. Note that this conformal coating is a temporary solution; we use it to determine its effectiveness. The future overmolding technique will result in more durable protection. The conformally coated PowerBlade passes the static force and drop tests in UL 2735 without damage, but the impact test does destroy the unit and expose live parts. The live parts do not extend to the edge, however, and therefore do not present a safety hazard when the unit is plugged in.

## 6. DISCUSSION

In this section, we discuss some limitations of the current design, explore some possible workarounds, and propose some future directions for improvement. In particular, the accuracy could be further improved, the wireless system could be better utilized, and interval data could be collected with periodic timestamps.

### 6.1 Improving Accuracy

We identify two changes that could be taken in future designs to improve accuracy. First, the MSP430 microcontroller software algorithm that integrates  $I_{SENSE}$  to obtain the current waveform could be changed. Although the present implementation provides a usable signal, we believe a hardware implementation may better address baseline drift. Second, the acquisition of the current and voltage waveforms could be more tightly synchronized. For example, if the samples are acquired with a separation of 500  $\mu$ s, that delay will introduce an measurement error of 6% on a 150 W resistive load. PowerBlade has a 22.2  $\mu$ s delay between current and voltage sampling, but synchronous acquisition of the signals would be ideal.

Although error in real power is only 1.13% for the resistive loads and 6.5% for household devices, PowerBlade’s error in power factor is often higher. Figure 12 shows the accuracy in power factor (which is actually accuracy in apparent power) decreases significantly at lower wattages. A similar effect is observed in the household loads. Real power is the metric used to assess utility charges, so we believe this to be the more important value, but we have yet to determine the source of the error in apparent power.

### 6.2 Wireless Communications

The advertisement-only communication model that PowerBlade employs presents two areas for improvement. First, any BLE receiver can eavesdrop on these broadcasts as the data are transmitted in clear-text, so data security is an obvious area of improvement. We have verified that a nearby smartphone can respond to a PowerBlade advertisement to open a BLE connection, showing that changes from the advertisement-only model are also possible.

## 6.3 Interval Metering

PowerBlade can store accumulated energy in non-volatile memory, allowing it to aggregate total load usage. However, this data is a scalar value representing total load since boot or since inception. PowerBlade could be much more useful if it could serve as a fine-grained interval meter, providing energy usage data broken down by periodic intervals—typically 1, 15, or 60 minutes in duration—that are synchronized in time with other meters and “wall” time as this allows better visibility into energy use over time.

To support interval metering, PowerBlade needs a reliable method of obtaining and keeping the time, likely a combination of a wireless time synchronization protocol and a real-time clock. The primary difficulty in adding a real-time clock (RTC) is limited long-term energy availability in this form factor. To that end, we have identified supercapacitors capable of storing sufficient energy to operate an RTC for extended periods [12]. We intend to explore the viability of interval metering in this form factor in future work.

## 7. CONCLUSIONS

The state-of-the-art in plug-load metering fails to provide consumers and corporations the detailed knowledge they need to understand and adjust their energy consumption patterns at a size, cost, power, and usability point that permits widespread adoption. While plug loads represent one of the faster growing segments of electrical loads, existing systems for measuring them remain too expensive, draw too much idle power, lack a wireless interface, and are often too large or too cumbersome to easily deploy.

To address the gap between emerging needs and existing solutions, we present PowerBlade, a new power/energy meter design that enables a new paradigm in metering by making the sensor so small and unobtrusive that it can be permanently attached to a plug rather than an outlet. PowerBlade accurately meters the power of a load in real-time and wirelessly transmits that data to nearby smartphones or gateways using a Bluetooth Low Energy radio. With a thickness of a mere  $1/16$ ”, PowerBlade is the first power meter that is truly plug-through. Realizing this diminutive form factor, however, requires revisiting all of the key design choices for a power meter.

In this paper, we introduce several new methods—voltage sensing, current sensing, and power supply miniaturization, among others—to realize a new metering design point. This design offers accuracy within 1.13% of ground truth on a resistive load and 6.5% on a selection of non-unity power factor household devices. Furthermore, we show that the system’s volume, cost, wireless capability, and safety combine to make a usable and deployable system. With this new design in hand, researchers, ratepayers, and regulators will be able to inexpensively gain new insights into electricity usage patterns, hopefully yielding smarter and more energy-efficient choices.

## 8. ACKNOWLEDGMENTS

We thank our shepherd, Jie Liu, and the anonymous reviewers for their helpful feedback. This work was supported in part by the TerraSwarm Research Center, one of six centers supported by the STARnet phase of the Focus Center Research Program (FCRP) a Semiconductor Research Corporation program sponsored by MARCO and DARPA. This material is based upon work supported by the National Science Foundation under grant CNS-1350967, by the NSF/Intel Partnership on Cyber-Physical System (CPS) Security and Privacy under Award proposal title “Synergy: End-to-End Security for the Internet of Things, NSF proposal No. 1505684.”, and by the Graduate Research Fellowship Program under grant number DGE-1256260. This work partially supported by generous gifts from Intel and Texas Instruments.

## 9. REFERENCES

- [1] ADE7753 energy metering IC. <http://www.analog.com/en/products/analog-to-digital-converters/integrated-special-purpose-converters/energy-metering-ics/ade7753.html>.
- [2] APS 3B series datasheet.  
[http://www.adaptivepower.com/Resources/Documents/APS\\_3B%20Series\\_Datasheet\\_1014.pdf](http://www.adaptivepower.com/Resources/Documents/APS_3B%20Series_Datasheet_1014.pdf).
- [3] Belkin conserve insight energy use monitor.  
<https://www.belkin.com/conserve/insight/>.
- [4] Coilcraft flyback transformers Y8844-AL.  
<http://www.coilcraft.com/pdfs/y8844.pdf>.
- [5] Electronic product design Inc. PLM-1.  
[http://www.epd.com/power\\_meters.html#PLM-1](http://www.epd.com/power_meters.html#PLM-1).
- [6] Kill-a-watt electricity use monitor.  
<http://www.p3international.com/products/p4400.html>.
- [7] LEM TT 100-SD current transformer.  
[http://www.lem.com/docs/products/tt100sd\\_e.pdf](http://www.lem.com/docs/products/tt100sd_e.pdf).
- [8] Linear Technology LTC5800 wireless mote-on-chip.  
<http://www.linear.com/product/LTC5800-WHM>.
- [9] LNK302 off-line switcher IC. [http://www.mouser.com/ds/2/328/lnk302\\_304-306-179954.pdf](http://www.mouser.com/ds/2/328/lnk302_304-306-179954.pdf).
- [10] Mill-Max discrete spring loaded contacts.  
<http://www.mill-max.com/assets/pdfs/024.pdf>.
- [11] Nordic Semiconductor Bluetooth Smart SoC.  
<https://www.nordicsemi.com/eng/Products/Bluetooth-Smart-Bluetooth-low-energy/nRF51822>.
- [12] Panasonic electric double layer capacitors.  
<http://media.digikey.com/pdf/Data%20Sheets/Panasonic%20Capacitors%20PDFs/EEC-EP0E333,EP0F333.pdf>.
- [13] SR086 adjustable off-line inductorless switching regulator.  
<http://ww1.microchip.com/downloads/en/DeviceDoc/SR086%20D080613.pdf>.
- [14] SR10 capacitor-coupled, switched shunt, (CCSS) regulator.  
<http://ww1.microchip.com/downloads/en/DeviceDoc/SR10%20B080613.pdf>.
- [15] Texas Instruments CC2420 RF transceiver.  
<http://www.ti.com/product/cc2420>.
- [16] Texas Instruments TPS62122 step-down converter.  
<http://www.ti.com/product/tps62122>.
- [17] Watts Up? Pro plug load meter.  
<https://www.wattsupmeters.com/secure/products.php?pn=0>.
- [18] Standard for safety in electric utility meters. Technical Report UL2735, UL, May 2013.
- [19] Electric power monthly with data for June 2015. Technical report, U.S. Energy Information Administration, aug 2015.
- [20] B. Campbell and P. Dutta. Gemini: A non-invasive, energy-harvesting true power meter. In Real-Time Systems Symposium (RTSS), 2014 IEEE, pages 324–333. IEEE, 2014.
- [21] R. Condit. Transformerless power supplies: Resistive and capacitive. <http://ww1.microchip.com/downloads/en/AppNotes/00954A.pdf>, 2004.
- [22] B. Coxworth. Flipit lets you charge devices from outlets that are in use. <http://www.gizmag.com/flipit-usb-charger/20024/>, 2011.
- [23] S. DeBruin, B. Campbell, and P. Dutta. Monjolo: An energy-harvesting energy meter architecture. In Proceedings of the 11th ACM Conference on Embedded Networked Sensor Systems, page 18. ACM, 2013.
- [24] S. Gupta, M. S. Reynolds, and S. N. Patel. ElectriSense: single-point sensing using EMI for electrical event detection and classification in the home. In Proceedings of the 12th ACM international conference on Ubiquitous computing, pages 139–148. ACM, 2010.
- [25] C. J. Hansen. Internetworking with Bluetooth Low Energy. GetMobile, 19(2), Apr 2015.
- [26] X. Jiang, S. Dawson-Haggerty, P. Dutta, and D. Culler. Design and implementation of a high-fidelity AC metering network. In Information Processing in Sensor Networks, 2009. IPSN 2009. International Conference on, pages 253–264. IEEE, 2009.
- [27] S. Kwatra, J. T. Amann, and H. M. Sachs. Miscellaneous energy loads in buildings. American Council for an Energy-Efficient Economy, 2013.
- [28] T. Schmid, D. Culler, and P. Dutta. Meter any wire, anywhere by virtualizing the voltage channel. In Proceedings of the 2nd ACM Workshop on Embedded Sensing Systems for Energy-Efficiency in Building, pages 25–30. ACM, 2010.
- [29] S. Tumanski. Induction coil sensors a review. Measurement Science and Technology, 18(3):R31, 2007.
- [30] T. Wu and M. Srivastava. Low-cost appliance state sensing for energy disaggregation. In Proceedings of the Fourth ACM Workshop on Embedded Sensing Systems for Energy-Efficiency in Buildings, pages 53–55. ACM, 2012.
- [31] L. Yerva, B. Campbell, A. Bansal, T. Schmid, and P. Dutta. Grafting energy-harvesting leaves onto the sensornet tree. In Proceedings of the 11th International Conference on Information Processing in Sensor Networks, IPSN '12, pages 197–208. ACM, 2012.